BULLETIN OF THE POLISH ACADEMY OF SCIENCES
TECHNICAL SCIENCES
Vol. 52, No. 3, 2004

Analytical electromagnetic field and forces calculation for linear, cylindrical and spherical electromechanical converters

D. SPAŁEK*

Institute of Theoretical and Industrial Electrotechnics, Silesian University of Technology, 10 Akademicka St, 44–100 Gliwice, Poland

Abstract. The paper deals with the problem of force and torque calculation for linear, cylindrical and spherical electromechanical converter. The electromagnetic field is determined analytically with the help of separation method for each problem. The results obtained can be used as test tasks for electromagnetic field, force and torque numerical calculations. The analytical relations for torque and forces are also convenient for analysis of material parameters influence on electromechanical converter work.

Keywords: electromagnetic forces, anisotropy, analytical solutions.

1. Introduction

The determination of forces induced by electromagnetic field in electromechanical converter is an important problem. For electromechanical converters the acting force or torque values play deciding role for users. Modern technologies enable us to construct electromechanical converters with parts having wide range of properties between them anisotropic. Especially, the induction motors — linear, cylindrical and spherically shaped have got often magnetically anisotropic parts. The magnetic anisotropy could increase the value of forces and torques arising in electromechanical converter. The intention of this paper is to present the analytical solutions for linear, cylindrical and spherical induction motor problems. Basing on the main equation for electromagnetic forces density there are presented and discussed forces and torques values acting in electromechanical converters. The analytical relations for force and torque are the base for material parameters influence analysis. The presented below solutions for anisotropic and isotropic cases for magnetic circuit of induction motor can be used as a test-task for numerical packages, too.

2. Force and torques in electromagnetic field

The first pair of Maxwell equations [1–3] take the well-known form

$$\operatorname{curl}\vec{E} = -\dot{\vec{B}} \quad \wedge \quad \operatorname{div}\vec{B} = 0. \tag{1}$$

The second pair of Maxwell equations can be presented in vector notation as follows

$$\operatorname{div}\vec{D} = \rho \quad \wedge \quad \operatorname{curl}\vec{H} = \vec{j} + \dot{\vec{D}}. \tag{2}$$

The constitutive relation for electromagnetic field vectors for non-hysteresis medium are

$$H_u = \nu_{uv} B_v, \tag{3}$$

$$D_u = \varepsilon_{uv} E_v, \tag{4}$$

where ε_{uv} denote dielectric permittivity, ν_{uv} are magnetic reluctivity, u, v, w are curvilinear system co-ordinates (summation due to twice appearing indices is accepted).

The volume density of the total force [4, 5] can be written in the form of (Appendix)

$$\vec{f} = \vec{f_L} + \vec{N} + \vec{M}, \tag{5}$$

that point out the physical reasons for arising of the electromagnetic force component and is widely used for calculation of forces that appear in electromagnetic field region [6–9]. On the right hand side of Eq. 5 there are three components of electromagnetic force as follows

— acting on external currents/charges — the Lorentz force equals to

$$\vec{f_L} = \rho\vec{E} + \vec{j} \times \vec{B}, \tag{6}$$

— originated by change of magnetic reluctivity and electric permittivity [10] — the so-called nonhomogenous component $\vec{N}$

$$\vec{N} = \frac{1}{2} B_u B_w \operatorname{grad}(\nu_{uw}) - \frac{1}{2} E_u E_w \operatorname{grad}(\varepsilon_{uw}), \tag{7}$$

and asymmetry component M. (Eq. 66).

The forces/torques described mathematically by Lorentz formula are called Lorentz forces/torques. The forces/torques given by non-homogeneous and asymmetry components are called material forces/torques.

The tensor notation — presented in Appendix — is convenient for forces components evaluation in curvilinear co-ordinate systems e.g. cylindrical and spherical. The total force density can be also presented with the help of Maxwell stress tensor in vector notation as follows

$$div(-e\vec{\sigma}_u) = ef_{Lu} + eN_u + eM_u, \tag{8}$$

where

$$\vec{\sigma}_u = -\vec{B}H_u + \vec{i}_u e_V, \tag{9}$$

$$f_{Lu} = j_v B_w - j_w B_v, \tag{10}$$

$$N_u = \frac{1}{2}\frac{\partial \nu_u}{e\partial u} B_u^2 + \frac{1}{2}\frac{\partial \nu_{uv}}{e\partial u} B_u B_v + \frac{1}{2}\frac{\partial \nu_{wv}}{e\partial u} B_v B_w + \frac{1}{2}\frac{\partial \nu_v}{e\partial u} B_v^2, \tag{11}$$

* email: Dariusz.Spalek@polsl.pl

$$M_u = \frac{1}{2}(\nu_{uv} - \nu_{vu})B_u \frac{\partial B_v}{e\partial u} + \frac{1}{2}(\nu_{vu} - \nu_{uv})B_v \frac{\partial B_u}{e\partial u}. \quad (12)$$

For Cartesian co-ordinate system $e = 1$, $u = x$ (Section 3); for cylindrical $e = r$, $u = \alpha$ (Section 4) and spherical system $e = r^2 \sin\vartheta$, $u = \varphi$ (Section 5), subsequently. So, the virtue of tensor notation is evident: it leads to the vector notation easily. Moreover, the tensor notation can be easily implemented in any programming language. The components of tensors —- presented in matrix form —- are very convenient in use for any loop algorithms, especially.

3. Linear electromechanical converter (1 — dimensional field)

The simplest linear electromechanical converter [11] for analytical analysis of electromagnetic field and force calculation is presented. For describing Lorentz F_L and anisotropy forces F_{Fe} the main Eq. (5) will be applied. The model of the electromechanical converter considered is an induction linear motor with conducting and anisotropic carriage (Fig. 1). The model can represent linear motor used in traction. The motor carriage is smooth and magnetically homogeneous. The conducting rotor carriage has the width a, and the air-gap width is $g = \text{const}$.

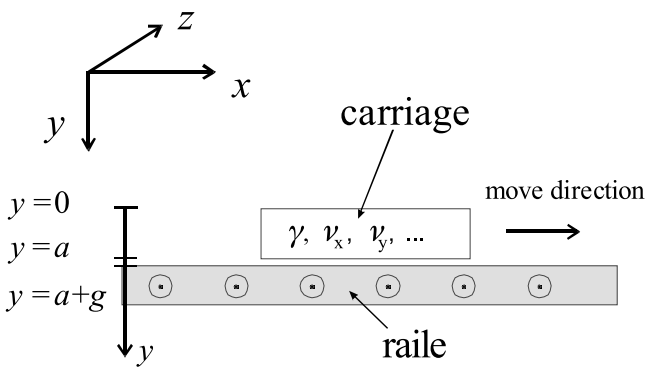

Fig. 1. Model of linear induction motor

For the linear induction motor the analytical solution for the electromagnetic field distribution and forces can be found. The correctness of the analytical analysis gives the possibility to demand for the highest accuracy of force values. Additionally, the solutions obtained for forces decomposition confirm the form of Eq. (5) mathematically proved (in Appendix) . The total force decomposition for components called is satisfied as shown in this paragraph.

The electromagnetic field calculation will be provided under the following assumptions

a) electric displacement current vanishes due to the small field frequency [11],
b) Maxwell's stress tensor part connected with the electric field can be omitted due to considered range of the frequency $D_u E_v \ll H_u B_v$,
c) rail windings induce the sinusoidal mmf (magnetomotive force [10], [12])

$$\Theta_s(x) = \Theta_s \cos(ky - 2\pi f t), \quad (13)$$

where Θ_s stands for magnitude of mmf, y is the position on the infinitely long carriage towards move direction, k propagation constant, f means stator supply frequency,

d) reluctivities for motor carriage, are as follows

$$\begin{bmatrix} \nu_x & \nu_{xy} \\ \nu_{yx} & \nu_y \end{bmatrix},$$

e) conductivity of motor carriage is γ (isotropic parameter).

The assumed symmetry of linear motor leads to the one-dimensional analysis. Field change in perpendicular direction to the move direction is neglected. The magnetic flux density of vertical component of magnetic potential A_z can be presented as follows

$$\vec{B} = \vec{i}_x \frac{\partial A_z}{\partial y} - \vec{i}_y \frac{\partial A_z}{\partial x}. \quad (14)$$

The magnetic field strength components for the anisotropic region can be shown in the form of

$$H_x = \nu_x B_x + \nu_{xy} B_y, H_y = \nu_{yx} B_x + \nu_y B_y. \quad (15)$$

The Maxwell equation

$$\text{curl}(\vec{H}) = \vec{j} = \gamma \vec{E} = -\gamma \dot{\vec{A}} \quad (16)$$

and Eqs. (14)–(16) lead to the main equation in the form of

$$\nu_y \frac{\partial^2 A_z}{\partial x^2} - (\nu_{xy} + \nu_{yx}) \frac{\partial^2 A_z}{\partial x \partial y} + \nu_x \frac{\partial^2 A_z}{\partial y^2} = \gamma \dot{A}_z. \quad (17)$$

The time-partial derivative of A_z as a multiplication of the operand $i\omega$ and the complex magnetic potential A at the steady state could be represented as follows

$$\dot{\vec{A}} \to i\omega \vec{A}, \quad (18)$$

where ω means carriage currents pulsation.

Equation (17) leads to either generalized Helmholtz differential equation for conducting carriage

$$\nu_y \frac{\partial^2 A}{\partial x^2} - (\nu_{xy} + \nu_{yx}) \frac{\partial^2 A}{\partial x \partial y} + \nu_x \frac{\partial^2 A}{\partial y^2} = i\omega\gamma A, \quad (19)$$

or the Laplace differential equation for the air-gap region

$$\frac{\partial^2 A}{\partial x^2} + \frac{\partial^2 A}{\partial y^2} = 0. \quad (20)$$

Equations (19) and (20) will be solved by the separation of the variables in the form

$$A = X(x)Y(y) = XY. \quad (21)$$

At the steady-state function $Y(y)$ for monoharmonic stator mmf has the given below form

$$Y(y) = \exp(-iky). \quad (22)$$

Rearranging the Eq. (19) with due to separation scheme for $X(x)$ and $Y(y)$ leads to differential equation for the

layer

$$\frac{d^2X}{dx^2} + ik\frac{\nu_{xy}+\nu_{yx}}{\nu_y}\frac{dX}{dx} - \left(\frac{\nu_x k^2}{\nu_y} + \beta^2\right)X = 0, \quad (23)$$

and for the air-gap Eq. (20) takes the form given below:

$$\frac{d^2X}{dx^2} - k^2X = 0. \quad (24)$$

The solutions of the Eqs. (23) and (24) are given in Table 1. The four unknown constants a_a, b_a, a_δ, b_δ can be evaluated by formulating the boundary conditions and there are grouped in Table 2.

The evaluation of magnetic field potential distribution is followed by the electromagnetic torque components analytical calculations. The Maxwell stress tensor leads to the total electromagnetic torque by means of the well-known formula

$$F = \nu_o \int\limits_{\partial V} B_\alpha B_r dS. \quad (25)$$

The electromagnetic torque component forced by machine rotor currents can be evaluated by the Lorentz's force density as follows

$$F_L = \int\limits_V j_z B_r dV. \quad (26)$$

The equation shows the total torque decomposition, which can be written in the shortened form of

$$F = F_L + F_{Fe}, \quad (27)$$

where F_{Fe} denotes the so-called material torque. This component is calculated with the help of the Eq. (12) as follows ($u = x$)

$$F_{Fe} = \int\limits_V M_x dV. \quad (28)$$

All torques are calculated for chosen linear motor. The accuracy of the calculation provided with Mathcad$^{\mathrm{TM}}$ equals to 10^{-15} (data shown in Fig. 2 are for SI Unit System).

Table 1
Solution of the differential equations

Region	anisotropic carriage — Eq. (23) (index a)	air-gap — Eq. (24) (index δ)
Solutions $X(x)$	$X(x) = a_a \exp(\lambda_1 x) + b_a \exp(\lambda_2 x)$	$X(x) = a_\delta \exp(kx) + b_\delta \exp(-kx)$
constants	a_a, b_a	a_δ, b_δ

Table 2
The boundary conditions for magnetic field

Boundary condition	Field excited by stator currents	Constants for solutions
Rail mmf $y = a + g$	$\nu_o B_{\delta y} = -\frac{\partial \Theta_s}{\partial y}$	$a_a = \Theta_s \nu_o^{-1}\{Ue^{\lambda_1(a+g)} - We^{\lambda_2(a+g)}\}^{-1}$
		$a_1 = ik\frac{\nu_{xy}+\nu_{yx}}{2\nu_y}$
		$a_0 = \sqrt{k^2\frac{\nu_x}{\nu_y} + \frac{i\gamma\omega}{\nu_y}}$
Carriage surface $y = a$	$B_{\delta x} = B_{ax}$	
	$\nu_o B_{\delta y} = \nu_y B_{ay} + \nu_{yx} B_{ax}$	$\lambda_{1,2} = -a_1 \pm \sqrt{a_1^2 + a_0^2}$
		$b_a = -a_a S, a_\delta = a_a U, b_\delta = a_a W$
Inner layer surface $y = 0$	$\nu_y B_y + \nu_{yx} B_x = 0$	where
		$S = \frac{\nu_y\lambda_1 + ik\nu_{yx}}{\nu_y\lambda_2 + ik\nu_{yx}}$
		$P = \frac{\nu_y}{k\nu_o}(\lambda_1 e^{\lambda_1 a} - S\lambda_2 e^{\lambda_2 a}) + \frac{i\nu_{yx}}{\nu_o}(e^{\lambda_1 a} - Se^{\lambda_2 a})$
		$Q = e^{\lambda_1 a} - Se^{\lambda_2 a}$
		$U = \frac{1}{2}(P+Q)e^{-ka}$
		$W = \frac{1}{2}(Q-P)e^{ka}$

Linear induction machine – anisotropic carriage (SI unit system)

$$\nu o := 4^{-1} \cdot \pi^{-1} \cdot 10^7$$

$$\nu x := \frac{\nu o}{3} \qquad \nu y := \frac{\nu o}{1.5} \qquad \nu xy := 0.5 \cdot \nu y + 0.0 \cdot \nu y \qquad \nu yx := 0.0 \cdot \nu y - 0.0 \cdot \nu y \cdot i$$

$$\gamma := 7 \cdot 10^6$$

$$a1 := \frac{\nu yx + \nu xy}{2 \cdot \nu y} \cdot k \cdot i \qquad s := 2 \cdot \pi \cdot i \cdot 10 \qquad a0 := \sqrt{k^2 \cdot \frac{\nu x}{\nu y} + \frac{\gamma \cdot s + s^2 \cdot \varepsilon}{\nu y}} \qquad k := 0.70$$

$$g := 0.005 \quad l := 10 \quad a := 0.1 \quad \theta s := 2000 \quad \lambda 1 := -a1 - \sqrt{a1^2 + a0^2} \quad \lambda 2 := -a1 + \sqrt{a1^2 + a0^2}$$

FORCE COMPONENTS

Maxwell method $\qquad x := a + 0.3 \cdot g$ $\qquad$ Lorentz and material force

$$F := 1 \cdot \mathrm{Re}(Hy\delta(x) \cdot \overline{Bx\delta(x)}) \qquad F = 1.234 \qquad F\_L := \mathrm{Im}(s) \cdot \gamma \cdot k \cdot l \cdot C \qquad F\_L = 1.244$$

$$F\_Fe := l \cdot k \cdot \mathrm{Im}\left[\int_0^a (\nu yx - \overline{\nu xy}) \cdot (Bxa(x) \cdot \overline{Bya(x)})dx\right]$$

Forces ratio

$$\frac{F\_L}{F} = 1.008 \qquad \frac{F\_Fe}{F} = -0.008 \qquad \frac{F\_L + F\_Fe}{F} = 1.000$$

Fig. 2. Torque calculations for anisotropic rotor — Mathcad$^{\mathrm{TM}}$ program

4. Cylindrical electromechanical converter (2 – dimensional field)

For describing Lorentz T_{eL} and anisotropy T_{eFe} torques the proved method for induction motor with solid rotor will be applied [12–15]. Let us consider the model of the induction motor with conducting and anisotropic rotor presented in Fig. 3. The model can represent the 2-phase ferrite induction machine widely used in the industry. The motor rotor is magnetically homogeneous, so the tangential component of non-homogeneous component vanishes $N_\alpha = 0$. The magnetic rotor does not exhibit hysteresis phenomenon. The machine rotor is cylindrical. Its outer radius is R. The conducting rotor layer has the width a, and the air-gap width is $g = \mathrm{const}$.

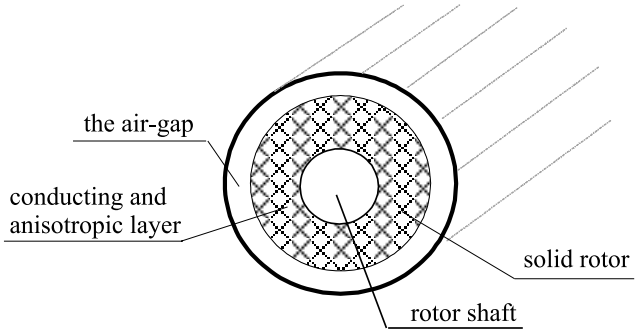

Fig. 3. Model of induction motor with solid rotor

For the simplified model of the induction motor the analytical solution for the electromagnetic field distribution can be found. The correctness of the provided analysis gives the possibility to demand for the accuracy almost of 100% for torque components values. The numerical analysis does not ensure such the level of torque calculations. The electromagnetic torque decomposition balance is satisfied, too.

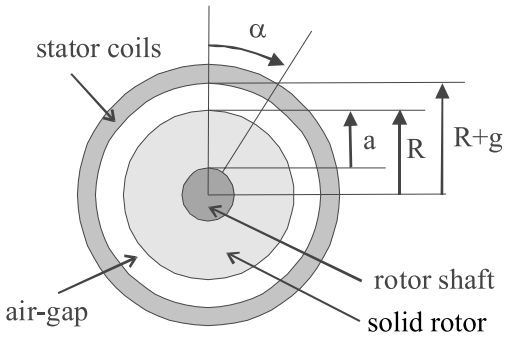

Fig. 4. Induction motor model — the cross-section and dimensions

The electromagnetic field calculation will be provided under the following assumptions

a) electric displacement current vanishes,
b) Maxwell's stress tensor part connected with the electric field can be omitted due to considered range of the frequency,
c) stator windings induce the sinusoidal $2p$-pole mmf

$$\Theta_s(\alpha) = \Theta_s \cos(p\alpha - 2\pi f t), \tag{29}$$

where Θ_s stands for the magnitude of mmf, α is the position angle, f means the stator supply frequency,
d) reluctivities for motor rotor, are given by the reluctivity matrix generally

$$\begin{bmatrix} \nu_r & \nu_{r\alpha} \\ \nu_{\alpha r} & \nu_\alpha \end{bmatrix}$$

e) conductivity of machine rotor is γ (isotropic parameter).

The assumed symmetry of motor geometry and mmf source lead to the two-dimensional analysis. The magnetic flux density in terms of an axial component of magnetic potential A_z (z is symmetry axis of solid rotor) can be presented as follows

$$\vec{B} = \vec{i}_r \frac{1}{r}\frac{\partial A_z}{\partial \alpha} - \vec{i}_\alpha \frac{\partial A_z}{\partial r}. \tag{30}$$

The magnetic field strength components for the anisotropic region can be shown in the general form of

$$H_r = \nu_r B_r + \nu_{r\alpha} B_\alpha, H_\alpha = \nu_{\alpha r} B_r + \nu_\alpha B_\alpha. \tag{31}$$

Combining the Maxwell equation with the Eqs. (30) and (31) one obtains for steady-state the differential Helmholtz equation for the anisotropic solid rotor

$$\frac{\nu_\alpha}{r}\frac{\partial}{\partial r}(r\frac{\partial A}{\partial r}) - \frac{\nu_{r\alpha}+\nu_{\alpha r}}{r}\frac{\partial^2 A}{\partial r \partial \alpha} + \frac{\nu_r}{r^2}\frac{\partial^2 A}{\partial \alpha^2} = i\omega\gamma A, \tag{32}$$

and Laplace differential equation for the air-gap

$$\frac{1}{r}\frac{\partial}{\partial r}(r\frac{\partial A}{\partial r}) + \frac{1}{r^2}\frac{\partial^2 A}{\partial \alpha^2} = 0. \tag{33}$$

The Eqs. (32) and (33) will be solved by the separation of the variables in the following form

$$A = R(r)S(\alpha) = RS, \tag{34}$$

at the steady-state when the function $S(\alpha)$ for monoharmonic stator mmf takes the form

$$\frac{d^2R}{dr^2} + \frac{[1-2c]}{r}\frac{dR}{dr} - \left[\frac{\nu_r p^2}{\nu_\alpha r^2} + \beta^2\right] R = 0, \tag{35}$$

where p is a pair-pole number for stator windings.

Equation (32) with respect to the given above separation scheme for the functions $R(r)$ and $S(\alpha)$ gives the differential equation for the layer

$$\frac{d^2R}{dr^2} + \frac{[1-2c]}{r}\frac{dR}{dr} - \left[\frac{\nu_r p^2}{\nu_\alpha r^2} + \beta^2\right] R = 0, \tag{36}$$

and for the air-gap

$$\frac{r}{R}\frac{d}{dr}\left(r\frac{dR}{dr}\right) = p^2. \tag{37}$$

The solutions of the Eqs. (36) and (37) [16] are grouped in Table 3. The four unknown constants a_a, b_a, a_δ, b_δ can be evaluated by formulating the boundary conditions and there are grouped in Table 4.

Table 3
Solution of the differential equations

Region	anisotropic layer — Eq. (36) (index a)	air-gap — Eq. (37) (index δ)
Solutions for $R(z)$, $z = \beta r$.	$R(z) = a_a z^c I_{pB}(z) + b_a z^c K_{pB}(z)$ $c = -ip(\nu_{\alpha r}+\nu_{r\alpha})/2\nu_\alpha$ $p_B = \sqrt{c^2 + p^2\nu_r/\nu_\alpha}$	$R(r) = a_\delta r^p + b_\delta r^{-p}$
constants	a_a, b_a	a_δ, b_δ

Table 4
The boundary conditions for magnetic field

Boundary condition	Field excited by stator currents	Constants for solutions
Stator current mmf $r = R + g = R_g$	$\nu_o B_{\delta\alpha} = -\frac{1}{R_s}\frac{\partial \Theta_s}{\partial \alpha}$	$a_a = \Theta_s \nu_o^{-1}\{UR_s^p - WR_s^{-p}\}^{-1}$ $b_a = -a_a S, a_\delta = a_a U, b_\delta = a_a W$ where
Rotor outer surface $r = R$	$B_{\delta r} = B_{ar}$, $\nu_o B_{\delta\alpha} = \nu_\alpha B_{a\alpha} + \nu_{\alpha r} B_{ar}$	$S = \frac{I'_{pB}(\beta R_a)}{K'_{pB}(\beta R_a)}, \beta = \sqrt{i\omega\gamma/\nu_\alpha}$ $P = \frac{\beta\nu_\alpha}{p\nu_o}\left(I'_{pB}(\beta R) - SK'_{pB}(\beta R)\right)$
Inner layer surface $r = R - a = R_a$	$\nu_\alpha B_\alpha + \nu_{\alpha r} B_r = 0$	$Q = I_{pB}(\beta R) - SK_{pB}(\beta R)$ $U = 0.5\left(PR^{-p+1} + QR^{-p}\right)$ $W = 0.5\left(-PR^{p+1} + QR^p\right)$

After evaluating the magnetic field potential distribution both the magnetic flux density components and the electromagnetic torque components can be evaluated, analytically. The Maxwell stress tensor leads to the total electromagnetic torque by means of the well-known formula

$$T_e = \nu_o r \int_{\partial V} B_\alpha B_r dS. \tag{38}$$

The electromagnetic torque component forced by machine rotor currents can be evaluated by Lorentz's force density as follows

$$T_{eL} = \int_V r j_z B_r dV. \tag{39}$$

There is a question: whether the both torques are equal for electromechanical converter which rotor exhibits the magnetic anisotropy features? According to Eq. (5) — after applying the Gaussian theorem [17] — for a cylindrical surface ∂V which is situated in the air-gap it is satisfied

$$T_e = T_{eL} + T_{eFe}. \tag{40}$$

The equation shows the total torque decomposition (non-homogeneous component vanishes), where T_{eFe} denotes the so-called material torque. The material torque can be physically interpreted as a part of total torque that can be exerted only if either directional nonhomogenity or forced magnetic anisotropy appears. The electromagnetic torques at the steady state are calculated exemplary electromechanical converter. The considered cases of the anisotropy are grouped in Table 5.

Table 5
Rotor magnetic anisotropy cases and results of calculations for the induction motor

$l = 0.3$, $R = 0.1$, $a = 0.07$, $\Theta s = 500$, $p = 2$, $\gamma = 7 \cdot 10^5$, $g = 0.001$, $s = 2\pi \cdot 3.0i$				
The case	The reluctivities $\nu_o = (4\pi 10^{-7}\ \mathrm{H/m})^{-1}$	The current torque ratio $T_{e,L}/T_e$ [%]	The material torque ratio $T_{e,Fe}/T_e$ [%]	The total torque value T_e [Nm]
a)	$\nu_r = \nu_\alpha = 0.04\nu_o$ $\nu_{r\alpha} = \nu_{\alpha r} = 0$	100,0	0,0	4,29
b)	$\nu_\alpha = 0.04\nu_o\ \nu_r = 0.05\nu_o$ $\nu_{r\alpha} = \nu_{\alpha r} = 0$	100,0	0,0	3,46
c)	$\nu_r = \nu_\alpha = 0.04\nu_o$ $\nu_{r\alpha} = \nu_{\alpha r} = 0.1\nu_r$	100,0	0,0	4,34
d)	$\nu_\alpha = 0.04\nu_o\ \ \nu_r = 0.05\nu_o$ $\nu_{r\alpha} = \nu_{\alpha r} = 0.1\nu_r$	100,0	0,0	3,50
e)	$\nu_\alpha = 0.04\nu_o\ \nu_r = 0.05\nu_o$ $\nu_{r\alpha} = 0.10\nu_r$ $\nu_{\alpha r} = 0.15\nu_r$	91,4	8,6	3,83
f)	$\nu_\alpha = 0.04\nu_o\ \nu_r = 0.05\nu_o$ $\nu_{r\alpha} = -0.10i\nu_r$ $\nu_{\alpha r} = +0.10i\nu_r$	100,0	0,0	4,01
g)	$\nu_\alpha = 0.04\nu_o\ \nu_r = 0.05\nu_o$ $\nu_{r\alpha} = \{0.10 - i0.10\}\nu_r$ $\nu_{\alpha r} = \{0.15 + i0.10\}\nu_r$	91,3	8,7	4,44

Induction motor with solid anisotropic rotor

$\nu r := \frac{\nu o}{30}$ $\nu\alpha := \frac{\nu o}{35}$ $\nu r\delta := \nu o$ $\nu\alpha\delta := \nu o$ $\nu rx\alpha := 0.1 \cdot \nu\alpha$ $\nu\alpha r := 0.2 \cdot \nu\alpha$

$c := -\frac{\nu\alpha r + \nu r\alpha}{2 \cdot \nu\alpha} \cdot p \cdot i$ $s := 2 \cdot \pi \cdot i \cdot 5$ $pB := \sqrt{p^2 \cdot \frac{\nu r}{\nu\alpha} + c^2}$ $p\delta := p \cdot \sqrt{\frac{\nu r\delta}{\nu\alpha\delta}}$ $p := 2$

$g := 0.0015$ $l := 0.35$ $R := 0.1$ $a := 0.07$ $\theta s := 800$ $\gamma := 9 \cdot 10^6$

$c = -0.3i$ $pB = 2.139$ $\beta = \sqrt{(s \cdot \gamma + s^2 \cdot \varepsilon) \cdot \nu\alpha^{-1}}$ $\beta := \sqrt{s \cdot \gamma \cdot \nu\alpha^{-1}}$

Torque components $r := R + 0.4g$

Maxwell method

$Te := r^2 \cdot \pi \cdot l \cdot \mathrm{Re}(H\alpha\delta(r) \cdot \overline{Br\delta(r)})$ $Te = 12.612$

Lorentz and material torques

$$TeL := p \cdot \pi \cdot l \cdot \mathrm{Im}(s) \cdot \gamma \cdot \int_{Ra}^{R} (|Aa(r)|)^2 \cdot rdr \qquad TeL = 12.451$$

$$TeFe := p \cdot \pi \cdot l \cdot \mathrm{Im}\left[\int_{Ra}^{R} (\nu\alpha r - \overline{\nu r\alpha}) \cdot \left(Bra(r) - \overline{B\alpha a(r)}\right) \cdot rdr\right] \qquad TeFe = 0.161$$

Torques ratios

$\frac{TeL}{Te} = 0.98723$ $\frac{TeFe}{Te} = 0.01277$ $\frac{TeL + TeFe}{Te} = 1.00000$

Fig. 5. Torque calculations for anisotropic rotor — Mathcad$^{\mathrm{TM}}$ program

From the analyses carried out and grouped in Table 5 it is apparent, that the material torque component can appear for induction motor with round, homogeneous and non-hysteresis rotor if the matrix of magnetic reluctivities is not Hermitan conjugate.

For the electromechanical converter the electromagnetic torque components have been evaluated — Fig. 5. It is significant that for induced anisotropy (the cases e) and g)) appears the material torque T_{eFe}. For Hermitian conjugate reluctivity matrix — case f) (or for symmetrical matrix particularly) the material torque vanishes.

Hence, *there is possible to express the total torque T_e (calculated by Maxwell stress surface integral) caused by Lorentz force in the form of surface integral for Hermitian conjugate reluctivity matrix (e.g. symmetrical matrix).*

For the analysis of influence of normal magnetic anisotropy ($\mu_{r\alpha} = \mu_{ar} = 0$) on the torque-slip curve shape there are considered three cases of rotor magnetic anisotropy

with radial-dominate magnetic reluctivity — Tr and $\mu_r > \mu_a$,

with angular-dominate magnetic reluctivity — $T\alpha$ and $\mu_a > \mu_r$,

compared with the case of isotropic rotor – T0.

For the three specified above cases (at the condition $\mu_r + \mu_\alpha = \text{const} = 30 \cdot \mu_o$, $\gamma = 7 \cdot 10^6$ S/m, $R = 0.05$ m, $a = 0.03$ m, $g = 0.001$ m, $\Theta = 500$ A, $p = 1$, $l = 0.3$ m, $f_1 = 50$ Hz) the electromagnetic steady-state torque-slip curve ($s = (f_1 - np)/f_1$) have been obtained with the help of the presented magnetic field distribution — Fig. 6.

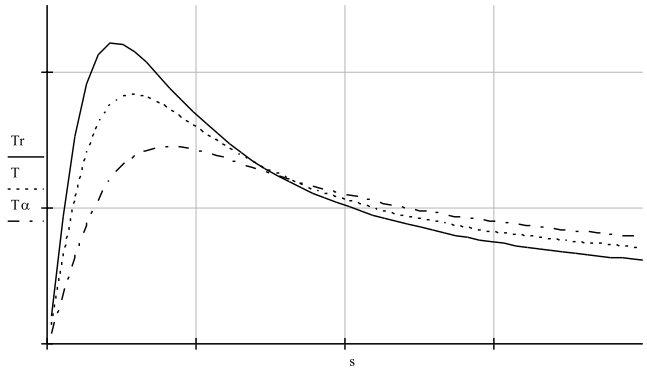

Fig. 6. Torque-slip curves for different anisotropy: Tr for $\mu_r > \mu_\alpha$ — solid line, T for $\mu_r = \mu_\alpha$ — dot line (isotropic rotor), $T\alpha$ $\mu_r > \mu_\alpha$ — dash-dot line (for all cases $\mu_r + \mu_a = \text{const}$, $\mu_{r\alpha} = \mu_{\alpha r} = 0$)

The analyses carried for cylindrically shaped electromechanical converter have brought out to the issues, such as

— For the electromechanical converter with round rotor, which does not exhibit both the nonhomogenity of magnetic reluctivity and the hysteresis phenomenon only the anisotropy of the magnetic reluctivity may cause the material torque. Indeed, the material torque appears for the cylindrical-shaped electromechanical converter in the case

$$\nu_{r\alpha} \neq \overline{\nu}_{\alpha r}$$

— For the electrical machine rotor with radial-dominate magnetic reluctivity the electromagnetic torque is the greatest one for stable ('arising') part of torque-slip curve.

— The obtained results enable one to state that the electromagnetic torque of electromechanical converter can be represented by the surface integral for both the isotropic and the normal magnetic anisotropy of rotor.

5. Spherical electromechanical converter (3 – dimensional field)

For the electromechanical converter with spherical rotor — Fig. 7 (e.g. spherical motor [18–22]) the electromagnetic field could be determined with the help of separation of variable method. The book [20] presents the main solutions for spherical converter by means of circuit analysis. The further works present the field analysis of the problem in theoretical form [18, 19] or numerical [21, 22].

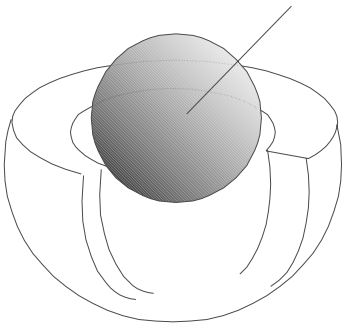

Fig. 7. Spherically shaped electromechanical converter-view

The non-standard separation proposed leads to the analytical solution for the spherical symmetry problem for anisotropic region. The solution obtained can be applied for analysis of electromechanical converters with spherically shaped moving part. The magnetic flux density for spherical co-ordinate can be presented in the form

$$\vec{B} = \frac{\vec{1}_r}{r\sin\theta}\left\{\frac{\partial A_\theta}{\partial\varphi} - \frac{\partial A_\varphi \sin\theta}{\partial\theta}\right\} - \frac{\vec{1}_\varphi}{r}\left\{\frac{\partial r A_\theta}{\partial r} - \frac{\partial A_r}{\partial\theta}\right\} + \frac{\vec{1}_\theta}{r\sin\theta}\left\{\frac{\partial}{\partial r} r A_\varphi \sin\theta - \frac{\partial A_r}{\partial\varphi}\right\}. \quad (41)$$

For simple case $\vec{A} = \vec{A}_\theta = A_\theta\vec{1}_\theta = A\vec{1}_\theta$ (is motivated physically by the construction of the spherical motor — Figs. 7 and 8) it is satisfied

$$\vec{B} = \frac{\vec{1}_r}{r\sin\theta}\left\{\frac{\partial A_\theta}{\partial\varphi}\right\} - \frac{\vec{1}_\varphi}{r}\left\{\frac{\partial r A_\theta}{\partial r}\right\}. \quad (42)$$

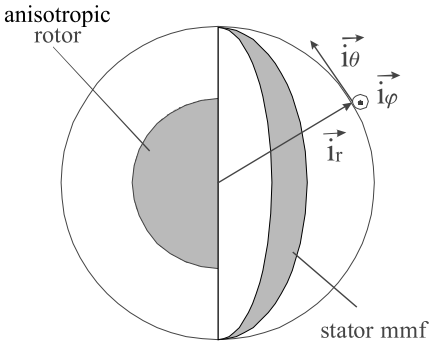

Fig. 8. Spherical co-ordinate system

The Maxwell's Eq. (16) and constitutive relation for field (42) in the form of

$$\begin{bmatrix} H_r \\ H_\varphi \\ H_\theta \end{bmatrix} = \begin{bmatrix} \nu_{rr}B_r + \nu_{r\varphi}B_\varphi \\ \nu_{\varphi r}B_r + \nu_{\varphi\varphi}B_\varphi \\ 0 \end{bmatrix} \tag{43}$$

lead for θ-component to the relation given below

$$\frac{1}{r}\frac{\partial}{\partial r}r\left(\frac{\nu_{\varphi r}}{r\sin\theta}\left\{\frac{\partial A_\theta}{\partial\varphi}\right\} - \frac{\nu_{\varphi\varphi}}{r}\left\{\frac{\partial rA_\theta}{\partial r}\right\}\right)$$
$$-\frac{1}{r\sin\theta}\frac{\partial}{\partial\varphi}\left(\frac{\nu_{rr}}{r\sin\theta}\left\{\frac{\partial A_\theta}{\partial\varphi}\right\} - \frac{\nu_{r\varphi}}{r}\left\{\frac{\partial rA_\theta}{\partial r}\right\}\right) = j_\theta. \tag{44}$$

The standard separation method in the well-known form of

$$A = A_\theta = R(r)\Theta(\theta)\Phi(\varphi) = R\cdot\Theta\cdot\Phi, \tag{45}$$

does not lead to the easily solvable equation, but the proposed below non-standard separation

$$A = A_\theta = R(r)F(\varphi,\theta) = R\cdot F, \tag{46}$$

results in an easy separable equation

$$\frac{\nu_{\varphi\varphi}}{rR}\frac{\partial^2 rR}{\partial r^2} + \frac{\nu_{rr}}{r^2F\sin^2\theta}\frac{\partial^2 F}{\partial\varphi^2}$$
$$-\left(\frac{\nu_{\varphi r}}{rR}\frac{\partial R}{\partial r} + \frac{\nu_{r\varphi}}{r^2R}\frac{\partial rR}{\partial r}\right)\frac{1}{F\sin\theta}\frac{\partial F}{\partial\varphi} = i\omega\gamma. \tag{47}$$

For the separated function $F(\varphi,\theta)$ it is assumed the separation with the constant p^2 in the form of

$$\frac{1}{F\sin^2\theta}\frac{\partial^2 F}{\partial\varphi^2} = -p^2 \tag{48}$$

with the analytical solution

$$F = A\exp(ip\varphi\sin\theta) + B\exp(-ip\varphi\sin\theta). \tag{49}$$

The solution (exemplary for constant $B = 0$ due to technical aspects) leads to equation

$$\frac{\partial^2 rR}{\partial r^2} - ip\left(\frac{\nu_{\varphi r}}{r}\frac{\partial R}{\partial r} + \frac{\nu_{r\varphi}}{r^2}\frac{\partial rR}{\partial r}\right) = \left(\frac{p^2\nu_{rr}}{r^2} + i\omega\gamma\right)R, \tag{50}$$

that confirms the proposed non-standard separation (46) is successful (the solution for $A = 0$ and $B \neq 0$ is obtained by substituting $p \to -p$).

The equation obtained has the analytical solution for anisotropic region as follows [16]

$$R(r) = (\beta r)^{h-\frac{1}{2}}\left(C_1 I_\delta(\beta r) + C_2 K_\delta(\beta r)\right), \tag{51}$$

where it was denoted

$$\beta^2 = \frac{i\gamma\omega - \varepsilon\omega^2}{\nu_\varphi}, \tag{52}$$

$$h = ip\frac{\nu_{r\varphi} + \nu_{\varphi r}}{2\nu_\varphi}, \tag{53}$$

$$\delta = \pm\sqrt{(h-\tfrac{1}{2})^2 + \frac{p^2\nu_r + ip\nu_{r\varphi}}{\nu_\varphi}}. \tag{54}$$

For the air-gap ($\gamma = 0$) it is satisfied

$$\frac{\partial^2 rR}{\partial r^2} - (\kappa+1)\kappa\frac{R}{r} = 0 \tag{55}$$

$$(\kappa+1)\kappa = p^2 \tag{56}$$

with the solution given below

$$R = R(r) = ar^{\kappa 1} + br^{\kappa 2}. \tag{57}$$

The analytical solution for the spherical motor can be presented in terms of separated function $R(r)$ and $F(\varphi,\theta)$ obtained with the help of separation proposed. The exemplary spherical induction motor with anisotropic and spherical rotor is considered and shown in Figs. 7 and 8. For the monoharmonic magnetomotive force of stator the magnetic field distribution and electromagnetic torque are calculated. The data for analysis are presented in Fig. 9 (radii notation is adequate to Fig. 4).

The accuracy for both partial differential solutions are checked and presented in Fig. 10 for conducting and nonconducting region for separated ordinary differential equations. The solutions for ordinary differential equation

Spherical induction motor with anisotropic rotor (SI units)

$\nu r := \frac{\nu o}{15}$ $\quad \nu\phi := \frac{\nu o}{20}$ $\quad \nu r\delta := \frac{\nu o}{1}$ $\quad \nu\phi\delta := \frac{\nu o}{1}$ $\quad \nu r\phi := 0.3\cdot\nu\phi$ $\quad \nu\phi r := 0.3\cdot\nu\phi$ $\quad p := 1$

$h := z\frac{\nu\phi r + \nu r\phi}{2\cdot\nu\phi}\cdot p\cdot i$ $\quad \lambda 1 := \sqrt{(0.5-h)^2 + (\nu r\cdot p^2 + z\cdot p\cdot i\cdot\nu r\phi)\cdot\nu\phi^{-1}}$ $\quad \lambda 2 := -\lambda 1$ $\quad \lambda := \lambda 1$ $\quad s := 2\cdot\pi\cdot i\cdot 10$

$g := 0.0002$ $\quad R := 0.045$ $\quad a := 0.03$ $\quad \theta s := 5000$ $\quad \gamma := 10\cdot 10^6$ $\quad \lambda = 1.22202$

Fig. 9. The data set for the exemplary spherical motor

$Z(\ )$ and $D(\ )$ denote solution for vector magnetic potential separated function $R(\ )$ for conducting region ($\gamma \neq 0$) and air-gap ($\gamma = 0$), respectively. In Fig. 10 LZ (RZ) means value of left-hand (right-hand) side of ordinary differential Eq. (50) for conducting region. In Figure 10 LD (RD) means value of left-hand (right-hand) sides of ordinary differential Eq. (55) for the air-gap region, respectively. The accuracy for both ordinary differential equations are checked and presented in Fig. 10, for exemplary data. For exact solutions it should be satisfied $LZ/RZ = 1$, and $LD/RD = 1$ as it is shown in Fig. 10.

$r := Ra + 0.5 \cdot a$ Accuracy for partial differential equations

$$LZ := \left[\frac{\partial^2}{\partial r^2} Z(\beta \cdot r) + \frac{2(l-h)}{r} r \frac{\partial}{\partial r}(Z(\beta \cdot r))\right] \quad RZ := \left[\beta^2 + \frac{\nu r \cdot p^2 + (z \cdot p \cdot i \cdot \nu r \phi)}{\nu\phi \cdot r^2}\right] \cdot Z(\beta \cdot r) \quad \frac{LZ}{RZ} = 1.00000$$

$$LD := \left[\frac{\partial}{\partial r}\left(\frac{\partial}{\partial r} D(r)\right) + \frac{2}{r} \cdot \frac{\partial}{\partial r} D(r)\right] \quad RD := \sqrt{p^2} r^2 \cdot \frac{\nu r \delta}{\nu\phi\delta} \cdot D(r) \quad \frac{LD}{RD} = 1.00000$$

Fig. 10. Accuracy for partial differential equations solutions

$r := R + 0.5 \cdot g$ Electromagnetic torque – total value

Maxwell's method $I\theta := 0.5 \cdot (\theta - \theta o)(\cos(\theta) - \cos(\theta o))$

Lorentz and material torques

$$Te := r^3 \cdot \pi \cdot I\theta \cdot \mathrm{Re}(H\phi\delta(r) \cdot \overline{Br\delta(r)}) \qquad Cr := \int_{Ra}^{R} (|Aa(r)|)^2 \cdot r^2 dr$$

$Te = 0.020$

$$TeCu := -z \cdot p \cdot \pi \cdot \gamma \cdot I\theta \cdot \mathrm{Im}(s) \cdot Cr$$

$TeCu = 0.020$

$$TeFe := p \cdot \pi \cdot I\theta \cdot \mathrm{Im}\left[\int_{Ra}^{R} (\nu\phi r - \overline{\nu r\phi}) \cdot (Bra(r) \cdot \overline{B\phi a(r)}) \cdot r^2 dr\right]$$

Torques ratios

$$\frac{TeCu}{Te} = 1.000 \qquad \frac{TeFe}{Te} = 0.000 \qquad \frac{TeCu + TeFe}{Te} = 1.00000$$

Fig. 11. Electromagnetic torque calculation for spherical motor

Power balance – Poynting vector, power losses, magnetic energy

$$Er := \frac{\overline{\nu r}}{2} \cdot k \cdot \int_{Ra}^{R} (|Z(\beta \cdot r) \cdot p|)^2 dr$$

$$E\phi := \frac{\overline{\nu\phi}}{2} \cdot k \cdot \int_{Ra}^{R} (|dxZ(\beta \cdot r)|)^2 dr$$

$$Ca := \begin{cases} 0 \text{ if } (\nu r\phi = 0) \cdot (\nu\phi r = 0) \\ -0.5 \cdot k \cdot z \cdot p \cdot i \cdot \left(\int_{Ra}^{R} Z(\beta \cdot r) \cdot \overline{dxZ(\beta \cdot r)} dr\right) \text{ otherwise} \end{cases}$$

$Er\phi := \overline{\nu r\phi} \cdot Ca \quad E\phi r := \overline{\nu\phi r} \cdot \overline{Ca}$

$E\mu := Er + E\phi + Er\phi + E\phi r$ $\quad E\varepsilon := 0.5 \cdot \varepsilon \cdot k \cdot (|s|)^2 \cdot Cr0$ $\quad Pq := (|s|)^2 \cdot \gamma \cdot k \cdot Cr0$

$E\mu := 0.01$ $\quad E\varepsilon := 0$ $\quad Pq := 1.238$

$Sc := \nu\phi\delta s \cdot k \cdot R \cdot D(R) \cdot \overline{dxD(R)}$ $\quad Q := 2 \cdot \mathrm{Im}(s \cdot E\mu + \overline{s} \cdot E\varepsilon)$ $\quad Pe := 2 \cdot \mathrm{Re}(s \cdot E\mu + \overline{s} \cdot E\varepsilon)$

$Sc = 1.238 + 1.309i$ $\quad Q = 1.309$ $\quad Pe = 0$

$$\frac{Er\phi + E\phi r}{Er + E\phi} = 0.078 \qquad \frac{E\varepsilon}{E\mu} = 0.000 \qquad \frac{Pq + Pe + Q \cdot i}{Sc} = 1.00000$$

Fig. 12. Electromagnetic field energy balance – calculation

For the evaluated magnetic filed distribution and electromagnetic torque has been calculated as shown in Fig. 11. There are presented the electromagnetic torques two components: Lorentz T_{eL} and material T_{eFe} that together constitute the total electromagnetic torque T_e. The torque decomposition is presented for checking analysis correctness, too. It should be pointed out that for either isotropic or normally anisotropic ($\nu_{\varphi r} = \nu_{r\varphi}$) rotor the anisotropy torque component disappears (in the case of Hermite conjugate reluctivity matrix, generally). The condition for this statement is the same as for cylindrically shaped rotor (Section 2).

Moreover, it was controlled accuracy of electromagnetic field solutions by means of the energy-power balance. The Poynting vector [1–5] is used for evaluating the magnetic energy and power losses in rotor. In order to check the accuracy of electromagnetic field solutions the energy-power balance has been checked. The Poynting vector is used for evaluating the magnetic energy and power losses in rotor. For checking the correctness of the obtained electromagnetic field distribution the power balance has been checked with the help of MathCad™ program. The complex power is calculated with the help of Poynting vector as follows

$$S_c = -i\omega\nu_o \int_S B_{\varphi\delta} A_z dS. \tag{58}$$

The fulfilment of electromagnetic field power balance ensures us that the analytical solutions are correct. Moreover, the power analysis leads to the power losses value in solid rotor

$$P_q = \gamma \int_V E_z^2 dV. \tag{59}$$

The exemplary calculations are shown in Fig. 12.

For technical purposes the analysis of influence of normal magnetic anisotropy ($\mu_{r\varphi} = \mu_{\varphi r} = 0$) on the torque-slip curve is carried out for two cases of rotor magnetic anisotropy

with radial-dominate magnetic reluctivity — Tr and $\mu_r > \mu_\varphi$,

with angular-dominate magnetic reluctivity — $T\phi$ and $\mu_\varphi > \mu_r$,

in comparison with the case of isotropic rotor — T.

For the three specified above cases (at condition $\mu_r + \mu_\varphi = \text{const} = 30 \cdot \mu_o$, $\gamma = 7 \cdot 10^6$ S/m, $R = 0.05$ m, $a = 0.03$ m, $g = 0.002$ m, $\Theta = 1000$ A, $p = 1$ — for radii notation see Fig. 4) the electromagnetic steady-state torque-slip curve have been obtained with the help of the presented magnetic field distribution — Fig. 13. The torque-slip curves show that electromechanical converter with radial-dominate magnetic reluctivity develops electromagnetic torque at stable part of torque-slip curve greater than for other anisotropy and isotropic rotor.

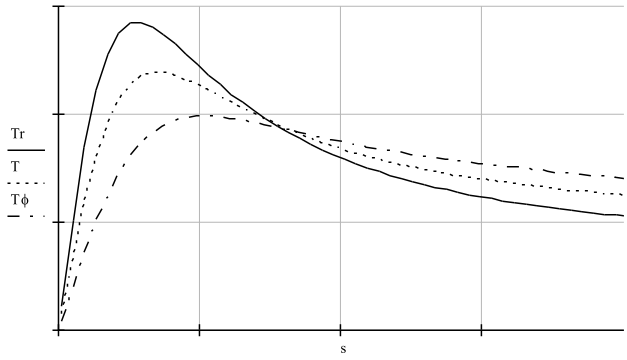

Fig. 13. Torque-slip curves for different anisotropy: Tr for $\mu_r > \mu_\varphi$ — solid line, T for $\mu_r = \mu_\varphi$ — dot line (isotropic rotor), $T\phi$ for $\mu_r > \mu_\varphi$ — dash-dot line (for all cases $\mu_r + \mu_\varphi = \text{const}$, $\mu_{r\varphi} = \mu_{\varphi r} = 0$) for spherical motor

6. Conclusions

The proposed method for electromagnetic torque/force calculation described in analytical way enables us to calculate its total and component values. The torque/force components indicate the physical reason for theirs

induction i.e Lorentz force and

material force component (nonhomogeneous and anisotropy components).

The mathematical proof for the main equation for force density has been provided with the help of tensor notation in Appendix. The tensor notation is convenient due to its mathematical form not only for curvilinear co-ordinate system but also for numerical algorithms.

For the chosen electromechanical converters linear, cylindrical and spherically shaped electromagnetic field and force/torque have been calculated. The accuracy of the calculation carried out has been checked by total force/torque decomposition correctness, too.

The solutions obtained lead to the conclusions that the radial-dominate anisotropy increases the electromagnetic torque value at steady-state of work.

For spherically shaped electromechanical converter the non-standard separation is proposed that leads to the analytical solutions. The mathematical form of non-standard separation is given by Eq. (46).

It is pointed out, that the Lorentz force can be presented by means of surface integral for homogeneous regions if its reluctivity matrix is either isotropic or anisotropic Hermite-conjugate.

Appendix

The energy tensor, which includes the stress tensor, can be defined as follows

$$\bar{\Im}_i^k = -G^{kl}F_{il} + \tfrac{1}{4}\delta_i^k G^{lm}F_{lm}. \tag{57}$$

The excitation tensor G^{ik} has the following form

$$G^{ik} = \nu_o F^{ik} + W^{ik},$$

where

$$W^{ik} = \begin{Bmatrix} 0 & -cP_x & -cP_y & -cP_z \\ cP_x & 0 & +I_z & -I_y \\ cP_y & -I_z & 0 & +I_x \\ cP_z & +I_y & -I_x & 0 \end{Bmatrix},$$

$$G^{ik} = \begin{Bmatrix} 0 & -cD_x & -cD_y & -cD_z \\ cD_x & 0 & -H_z & +H_y \\ cD_y & +H_z & 0 & -H_x \\ cD_z & -H_y & +H_x & 0 \end{Bmatrix}.$$

The tensor density of the energy tensor can be defined as follows

$$\bar{\Im}_i^k = -\mathbf{G}^{kl}F_{il} + \tfrac{1}{4}\delta_i^k \mathbf{G}^{lm}F_{lm}, \tag{58}$$

The first pair of the Maxwell's equations for the curvilinear co-ordinate system can be written in the form

$$F_{ik,l} + F_{kl,i} + F_{li,k} = 0. \tag{59}$$

The second pair of the Maxwell's equations where the tensor density of the excitation tensor appears has the form

$$\frac{\partial \mathbf{G}^{ik}}{\partial x^k} = \mathbf{G}^{ik}_{,k} = -\mathbf{j}^i. \tag{60}$$

Due to the skew-symmetry of tensors F^{ik} and G^{ik} one gets

$$F_{ik,l}\mathbf{G}^{ik} + 2\mathbf{K}_l + 2(F_{kl}\mathbf{G}^{ik})_{,i} = 0.$$

where

$$\mathbf{K}_l = F_{li}\mathbf{j}^i, \quad \mathbf{K}_l = \sqrt{|g|}K_l.$$

The excitation tensor and the electromagnetic field tensor are connected by material parameters as follows

$$\mathbf{G}^{ik} = \lambda^{ik}_{pq}F^{pq} + \Delta\mathbf{G}^{ik}, \tag{61}$$

where the material coefficients constitute the tensor

$$\lambda^{ik}_{pq} = \sqrt{g}\lambda^{ik}_{pq}.$$

The material relation (63) took the form known for $\Delta\mathbf{G}^{ik} = 0$ and for symmetrical material coefficients.

Consecutive, it can be written

$$(F_{ik}\mathbf{G}^{ik})_{,l} = F_{ik}\mathbf{G}^{ik}_{,l} + F_{ik,l}\mathbf{G}^{ik}, \tag{62}$$

hence, according to the Eqs. (61) and (62), there are satisfied the following relations:

$$(F_{ik}\mathbf{G}^{ik})_{,l} = \lambda^{pqik}F_{pq}F_{ik,l} + \lambda^{ikpq}F_{pq}F_{ik,l} + F_{ik}\lambda^{ik}_{pq,l}F^{pq} + [F_{ik}\Delta\mathbf{G}^{ik}_{,l} + F_{ik,l}\Delta\mathbf{G}^{ik}].$$

The material tensor λ^{pqik} in terms of the symmetrical and the asymmetrical parts can be represented as follows:

$$\lambda^{pqik} = \tfrac{1}{2}(\lambda^{pqik} + \lambda^{ikpq}) + \tfrac{1}{2}(\lambda^{pqik} - \lambda^{ikpq}) = \overset{pqik}{\underset{s}{\lambda}} + \overset{pqik}{\underset{a}{\lambda}}.$$

Hence

$$(F_{ik}\mathbf{G}^{ik})_{,l} = 2\mathbf{G}^{ik}F_{ik,l} - 4\mathbf{M}_l - 4\mathbf{Q}_l - 4\mathbf{N}_l,$$

where there were defined

$$\mathbf{Q}_l = -\tfrac{1}{2}[F_{ik}\Delta\mathbf{G}^{ik}_{,l} - F_{ik,l}\Delta\mathbf{G}^{ik}], \tag{63}$$

$$\mathbf{M}_l = -\tfrac{1}{2}\overset{ikpq}{\underset{a}{\lambda}}F_{pq}F_{ik,l} = \tfrac{1}{2}\lambda^{ik}_{\underset{a}{pq}}F^{pq}F_{ik,l}, \tag{64}$$

$$\mathbf{N}_l = -\tfrac{1}{2}F_{ik}\lambda^{ik}_{pq,l}F^{pq}. \tag{65}$$

The tensor force density satisfies the following relations:

$$\tfrac{1}{2}(F_{ik}\mathbf{G}^{ik})_{,l} + 2\mathbf{N}_l + 2\mathbf{Q}_l + 2\mathbf{M}_l + 2\mathbf{K}_l + 2(F_{kl}\mathbf{G}^{ik})_{,i} = 0,$$

thus finally with the help of Kronecker's delta symbol:

$$\mathbf{K}_l = -\{-\mathbf{G}^{kp}F_{lp} + \tfrac{1}{4}\delta_l^k\mathbf{G}^{pq}F_{pq}\}_{,k} - \mathbf{N}_l - \mathbf{Q}_l - \mathbf{M}_l.$$

The divergence of the energy tensor is equal to

$$\underline{(\bar{\Im}_i^{\ k})_{,k} = \mathbf{K}_i + \mathbf{N}_i + \mathbf{Q}_i + \mathbf{M}_i}, \tag{66}$$

The non-vector notation for the tensor density of generalised force volume density enables one to exchange the volume integral into the surface one with the help of Gauss's theorem.

References

[1] R. S. Ingarden and A. Jamiołkowski, *Classical Electrodynamics*, Elsevier-PWN, Warsaw, 1985.

[2] G. Joos, *Lehrbuch der Theoretischen Physik*, Leipzig, 1954, (in German).

[3] I. E. Tamm, *The Fundamentals of Electric Theory*, WNT, Warszawa, 1965, (in Polish).

[4] L. D. Landau and E. M. Lifszyc, *The Classical Theory of Fields*, Pergamon, New York, 1951.

[5] L. D. Landau and E. M. Lifszyc, *Electrodynamics Continuous Regions*, PWN 1960, (in Polish).

[6] Z. Ren, "Comparison of different force calculation method in 3D finite element modelling", *IEEE Transaction on Magnetics* 30(5), 3471–3474 (1994).

[7] R. Rosensweig, *Ferrohydrodynamics*, Cambridge University Press, Cambridge 1985.

[8] D. Spałek, "Anisotropy component of electromagnetic torque in electrical machines", *Archives of Electrical Engineering* 1, 109–126 (1999).

[9] D. Spałek, "Fast analytical model of induction motor for approaching rotor eccentricity", *COMPEL International Journal for Computation Mathematics in Electrical* & Electronics Engineering 18(4), MCB University Press, 570–586 (1999).

[10] B. Adkins and P. G. Harley, *The General Theory of Alternating Current Machines*, Chapman and Hall, London, 1978.

[11] J. Turowski, K. Zakrzewski and R. Sikora, *Analysis and Synthesis of Electromagnetic Field*, Ossolineum, Warszawa, 1990 (in Polish).

[12] Kent R. Davey, "Analytic analysis of single and three phase induction motors", *Problem 30a, Workshop TEAM*, http://ics.ec-lyon.fr/team.html.

[13] A. Nethe, T. Scholz and H-D. Stahlmann, "An analytical solution method for magnetic fields using the Fourier analysis and its application of ferrofluid driven electric machines", *Conference Proceedings ISTET 2003*, Warsaw, Vol. II, 421–424 (2003).

[14] A. Demenko, *Numerical Approach to Electrical Machines Dynamics*, Poznań University of Technology, Poznań, 1997 (in Polish).

[15] A. Demenko, "Finite element analysis of electromagnetic torque saturation harmonics in a squirrel cage machine", *COMPEL* 18(4), 619–628, (1999).

[16] I. S. Gradsztajn and I. M. Ryzik, *Tablicy Intjegralow, Sum, Rjadow i Proizwjedjenij*, Moskwa, 1962, (in Russian).

[17] S. Kästner, *Vectors, Tensors, Spinors*, Akademie-Verlag, Berlin, 1960 (in German).

[18] K. Davey, G. Vachtsevanos and R. Powers R., "The analysis of fields and torques in spherical induction motors", *IEEE Transaction on Magnetics* Mag-23 (1), (1987).

[19] J. Purczyński and L. Kaszycki, "Power losses and electromagnetic torque of spherical induction motor", *Rozprawy Elektrotechniczne* 34(3), 819–838 (1988) (in Polish).

[20] A. N. Miliach, *Osnowy Tjeorii Elektrodinamiczjeskich Sistjem s Tremija Stepjenjami Swobody Dwizjenija*, Akadjemija Nauk Ykrainskoj SSR, Kijew, 1956.

[21] K.-M. Lee, R. Roth and Z. Zhou, "Dynamic modelling and control of a ball-joint-like variable reluctance spherical motor", *ASME Journal Of Dynamics Systems, Measurements, And Control* 118(1), 29–40 (1996).

[22] Z. Zhou and K.-M. Lee, "Characterization of a three degrees-of-freedom variable-reluctance spherical motor", *J. of Systems Engineering* 4, 60–69 (1994) (also presented in *Proceedings of Japan-U.S.A. Symposium On Flexible Automation, Kobe, Japan*, July 11–18, 1994).